Brain Structure and Function
https://doi.org/10.1007/s00429-021-02429-y

ORIGINAL ARTICLE

The impact of Alzheimer's disease susceptibility loci on lateral ventricular surface morphology in older adults

Shan Li[1] · Na An[1] · Nan Chen[1] · Yin Wang[1] · Lin Yang[1] · Yalin Wang[2] · Zhijun Yao[1] · Bin Hu[1,3,4,5]

Received: 22 January 2021 / Accepted: 13 November 2021

Abstract

The enlargement of ventricular volume is a general trend in the elderly, especially in patients with Alzheimer's disease (AD). Multiple susceptibility loci have been reported to have an increased risk for AD and the morphology of brain structures are affected by the variations in the risk loci. Therefore, we hypothesized that genes contributed significantly to the ventricular surface, and the changes of ventricular surface were associated with the impairment of cognitive functions. After the quality controls (QC) and genotyping, a lateral ventricular segmentation method was employed to obtain the surface features of lateral ventricle. We evaluated the influence of 18 selected AD susceptibility loci on both volume and surface morphology across 410 subjects from Alzheimer's Disease Neuroimaging Initiative (ADNI). Correlations were conducted between radial distance (RD) and Montreal Cognitive Assessment (MoCA) subscales. Only the C allele at the rs744373 loci in *BIN1* gene significantly accelerated the atrophy of lateral ventricle, including the anterior horn, body, and temporal horn of left lateral ventricle. No significant effect on lateral ventricle was found at other loci. Our results revealed that most regions of the bilateral ventricular surface were significantly negatively correlated with cognitive scores, particularly in delayed recall. Besides, small areas of surface were negatively correlated with language, orientation, and visuospatial scores. Together, our results indicated that the genetic variation affected the localized areas of lateral ventricular surface, and supported that lateral ventricle was an important brain structure associated with cognition in the elderly.

Keywords Lateral ventricle · Genetic · Morphology · Alzheimer's disease · sMRI

Introduction

Alzheimer's disease (AD) is the most common neurodegenerative disease in elderly, which is characterized by the progressive decline of memory and cognition (Association 2019). With the accelerated process of the ageing population, there has been a rapid increase in the number of AD patients. The estimated number of AD patients would grow to 130 million by 2050 (Shah et al. 2016). Structural

Data used in preparation of this article were obtained from the Alzheimer's Disease Neuroimaging Initiative (ADNI) database (adni.loni.usc.edu). As such, the investigators within the ADNI contributed to the design and implementation of ADNI and/or provided data but did not participate in analysis or writing of this report. A complete listing of ADNI investigators can be found at: http://adni.loni.usc.edu/wp-content/uploads/how_to_apply/ADNI_Acknowledgement_List.pdf.

✉ Zhijun Yao
yaozj@lzu.edu.cn

✉ Bin Hu
bh@lzu.edu.cn

[1] Gansu Provincial Key Laboratory of Wearable Computing, School of Information Science and Engineering, Lanzhou University, No. 222 South Tianshui Road, Lanzhou 730000, Gansu Province, People's Republic of China

[2] School of Computing, Informatics, and Decision Systems Engineering, Arizona State University, Tempe, AZ, USA

[3] CAS Center for Excellence in Brain Science and Intelligence Technology, Shanghai Institutes for Biological Sciences, Chinese Academy of Sciences, ShangHai, China

[4] Joint Research Center for Cognitive Neurosensor Technology of Lanzhou University and Institute of Semiconductors, Chinese Academy of Sciences, LanZhou, China

[5] Engineering Research Center of Open Source Software and Real-Time System, Ministry of Education, Lanzhou University, Lanzhou, China

Published online: 14 January 2022

magnetic resonance imaging (MRI) has been applied in cognitive neuroscience as a stabilization tool, which has an ability to describe the high-resolution neuroanatomical information across the brain. Morphological changes of the brain in AD patients are well-recognized, including the hippocampus (Apostolova et al. 2012), amygdala (Poulin et al. 2011), ventricle (Apostolova et al. 2012), and the cortex (Frisoni et al. 2007). Both volume and surface have persistent changes and are considered as reliable biomarkers for predicting the incipient AD in mild cognitive impairment (MCI) patients (Guo et al. 2020; Ewers et al. 2012).

Lateral ventricle is a C-shaped cavity locates in the deep brain (Rhoton 2002) and can be divided into four subregions: anterior horn, body, occipital horn, and temporal horn (Barami et al. 2009). Current theory suggests that cerebrospinal fluid (CSF) Aβ-42, total tau, and phosphor-tau181 are the main available AD biomarkers for clinical diagnosis (Veitinger et al. 2014), and CSF is secreted in the ventricle (Alimajstorovic et al. 2020). The enlargement of lateral ventricular volume is a common pathological change in patients with AD, which is caused by the shrinkage of brain parenchymal and abnormal build-up of CSF (Apostolova et al. 2012; Bae et al. 2019). Specifically, the annual rate of expansion in ventricular volume was about 9% in AD patients, while 2% in healthy elderly (de Leon et al. 1989). The volume-based approach can reflect the overall change and the surface-based method can describe deformation detail of surface (Gutman et al. 2013; Wang et al. 2009; Shi et al. 2015). The surface-based method could facilitate further studies on the interactions between lateral ventricle and surrounding structures.

Genetic studies have identified that many genes were associated with the AD. Large scale genome-wide associated studies (GWAS) have revealed several AD genetic risk factors, such as *ApoE, CLU, CR1, CD33, BIN1, PICALM, CD2AP, NYAP1,* and others (Karch and Goate 2015; Lambert et al. 2013; Bertram et al. 2008; Beecham et al. 2009; Kunkle et al. 2019). Some susceptibility loci (*ApoE*, rs983392 within *MS4A6A,* rs11218343 within *SOLR1*, rs6733839 within *BIN1*, etc.) were found to be associated with MRI measures (cortical thickness, cortical surface area, and cortical volumes, subcortical structure volume, etc.) (Li et al. 2017; Chauhan et al. 2015; van der Meer et al. 2020; Grasby et al. 2020; Hofer et al. 2020) and brain metabolism (Stage et al. 2016), while the relationship between surface morphological changes and AD risk allele was relatively less to be reported. Some researches demonstrated that greater deformation of the hippocampal morphometry was observed when comparing *ApoE* E4 heterozygotes and homozygotes with non-carriers in longitudinal datasets (Crivello et al. 2010), especially the left hippocampus (Li et al. 2016). Previous studies have investigated the effects of *ApoE* E4 and *CLU* (rs11136000 and rs1532278) loci on ventricular expansion (Roussotte et al. 2014a, b). Their results indicated that these risk alleles were related to the faster ventricular expand bilaterally, and the effect of genes on the lateral ventricular surface was regionalized.

The lateral ventricle is one of the most affected anatomical structures in the development of AD, but most of the previous studies focused on the hippocampus, amygdala, and parietal lobe, etc. We speculated that risk genes would strongly influence the ventricular morphology and accelerate the development of AD. The lateral ventricle as a cavity has no responsible cognitive function, but it is highly correlated with changes in surrounding structures, such as hippocampus, thalamus, etc. Therefore, the relationship between lateral ventricular surface and cognitive function indirectly reflects the role of adjacent structures in different cognitive functions. In this study, volume-based analysis was used to detect the overall change of ventricular morphology, and the ventricular morphometry analysis system (VMAS) was used to assess the deformation detail of ventricular surface. Besides, we calculated the correlations between morphological features of lateral ventricular surface and Montreal Cognitive Assessment (MoCA) subscales. To sum up, the present study had two main purposes. First, to evaluate the presence of the risk allele that significantly affected the lateral ventricular morphology in 18 selected susceptibility loci in the elderly. Second, the relationship between adjacent structures of lateral ventricles and different cognitive functions was investigated.

Experimental procedures

Alzheimer's disease neuroimaging initiative

Data used in the preparation of this article were obtained from the Alzheimer's Disease Neuroimaging Initiative (ADNI) database (adni.loni.usc.edu). The ADNI was launched in 2003 as a public–private partnership, led by Principal Investigator Michael W. Weiner, MD. The primary goal of ADNI has been to test whether serial magnetic resonance imaging (MRI), positron emission tomography (PET), other biological markers, and clinical and neuropsychological assessment can be combined to measure the progression of mild cognitive impairment (MCI) and early Alzheimer's disease (AD). For up-to-date information, see www.adni-info.org.

The ADNI study was approved by the local Institutional Review Board, and all participants signed the informed consent prior to the collection of data. The current study was a cross-sectional design. After the procedure of genotyping, preprocessing, and segmentation, the scan which had technical failure during segmentation were excluded. We finally identified 410 participants

in this research, including 239 MCI (131 female, 108 male, 70.73 ± 7.11 years), 152 NC (92 female, 60 male, 74.08 ± 7.15 years), and 19 AD (13 female, 6 male, 74.65 ± 7.25 years). The chi-squared test showed no significant difference on gender ($p = 0.332$) between the three clinical stages. All subjects were asked to complete the MoCA. Inclusion and clinical diagnosis criteria for ADNI have been described in the ADNI manual (www.adni-info.org.). The Mini-Mental State Exam (MMSE) score of AD subjects were measured in 20–26 (inclusive), Clinical Dementia Rating Scale (CDR) scores of 0.5 or 1.0, and all subjects meet National Institute of Neurological and Communicative Diseases and Stroke/Alzheimer's Disease and Related Disorders Association (NINCDS/ADRDA) criteria for probable AD. MCI subjects had MMSE scores between 24 and 30 (inclusive), a memory complaint, have objective memory loss measured by education adjusted scores on Wechsler Memory Scale Logical Memory II, a CDR of 0.5, the absence of significant levels of impairment in other cognitive domains, essentially preserved activities of daily living, and the absence of dementia. NC subjects had MMSE scores between 24 and 30 (inclusive), a CDR of 0, non-depressed, non-MCI, and nondemented.

Genotyping and SNP selection

Single-nucleotide polymorphism (SNP) genotypes of subjects were generated by BeadStudio 3.2 software (Illumina) and have been uploaded to the ADNI website (Saykin et al. 2010). PLINK 1.9 (http://www.cog-genomics.org/plink/1.9/) was used to quality controls (QC) and extract the information of selected SNP except *ApoE* (Purcell et al. 2007), since *ApoE* genotyping of participants had been done at the screening visit and uploaded to the website by ADNI, as described in previous publication (Saykin et al. 2010). The procedure of QC included the following criteria: Hardy–Weinberg equilibrium (HWE) > 0.001, minor allele frequencies (MAF) > 0.05, and minimum call rates > 0.95.

We ultimately selected 18 genetic loci which have been previously reported as risk factors for Alzheimer's Disease (AD), including *ApoE*, *BIN1*-rs744373, *CLU*-rs7012010, *PICALM*-rs3851179, *MS4A6A*-rs920573, *CR1*-rs3818361, *CR1*-rs6691117, *HLA-DRB1*-rs9271246, *EPHA1*-rs11771145, *EPHA1*-rs11767557, *PTK2B*-rs1879189, *ABCA7*-rs3764650, *CD2AP*-rs9296562, *CD33*-rs3865444, *CD33*-rs3826656, *SORL1*-rs2070045, *NYAP1*-rs12539172, *MEF2C*-rs190982(Wang et al. 2017; Karch and Goate 2015; Bertram et al. 2008; Beecham et al. 2009; Ma et al. 2014b; Liu et al. 2017; Kunkle et al. 2019). Details of the gene information are presented in Table 1.

Table 1 Information of the selected SNP

Gene	SNP	Chr.	Position	Major/minor alleles	MAF
ApoE	ε4				
BIN1	rs744373	2	127894615	C/T	0.32
CLU	rs7012010	8	27448729	T/C	0.30
PICALM	rs3851179	11	85868640	G/A	0.35
MS4A6A	rs920573	11	59924959	G/A	0.38
CR1	rs3818361	1	207784968	C/T	0.20
	rs6691117	1	207782931	A/G	0.24
HLA-DRB1	rs9271246	6	32580084	G/A	0.24
EPHA1	rs11771145	7	143110762	G/A	0.37
	rs11767557	7	143109139	T/C	0.19
PTK2B	rs1879189	8	27198884	A/G	0.15
ABCA7	rs3764650	19	1046520	T/G	0.09
CD2AP	rs9296562	6	47490193	A/G	0.41
CD33	rs3865444	19	51727962	G/T	0.27
	rs3826656	19	51726613	A/G	0.25
SORL1	rs2070045	11	121448090	T/G	0.23
NYAP1	rs12539172	7	100091795	C/T	0.26
MEF2C	rs190982	5	88223420	A/G	0.36

SNP single-nucleotide polymorphism; *Chr.* chromosome; *MAF* minor allele frequencies

MRI acquisition

The detail of MRI acquisition parameters has been described elsewhere (Jack et al. 2008). In brief, high-resolution 3D T1 weighted MRI scans were acquired at multi-site, using 1.5 T MRI scanners (repetition time/echo time = 2400/1000 ms, flip angle = 8°, acquisition matrix size = 256 × 256 × 166, and reconstructed voxel resolution = 0.94 × 0.94 × 1.2 mm^3). For now, MRI is still the most common and reliable method for detecting brain abnormalities. Multi-site has minimal impact on morphological analysis (Jovicich et al. 2013). ADNI has done a lot to enhance standardization across sites and platforms of images acquired.

Segmentation of the lateral ventricles

First, the T1-weighted structural MRI of each subject were first linearly registered to the MNI152 space using FSL FLIRT (Smith et al. 2004), since FSL FLIRT has a much lower registration error rate on multi-site data and not affected by the signal-to-noise ratio (SNR) (Dadar et al. 2018). Second, all registered images were segmented into gray matter (GM), white matter (WM), and cerebrospinal fluid (CSF) using the CAT12 (http://www.neuro.uni-jena.de/cat/) within SPM12. Third, we applied the geodesic shooting algorithm (Ashburner and Friston 2011) to obtain a group-wise CSF template, which allowed us to extract the

group-wise ventricular template based on the CSF template using Automatic Lateral Ventricle delineation (ALVIN) binary mask (Kempton et al. 2011). Fourth, we visually inspected the ventricular boundaries of binary ventricular template, and wrapped the ventricular template back to the individual space using the deformation matrices from the estimation of group-wise CSF template. Fifth, ventricular surface meshes were reconstructed according to the shape of each individual ventricular volumetric template. Then, the ventricular structures of each subject were segmented from the MRI data. All the segmentation steps after registration were completed in SPM, and the method was described in more comprehensive detail in previous studies (Dong et al. 2020; Shi et al. 2015). In addition, total intracranial volume (TIV) and bilateral lateral ventricular volumes were obtained from MRI images via Freesurfer software (http://surfer.nmr.mgh.harvard.edu), which have been confirmed that has higher accuracy, good reproducibility, and sensitivity for automatically segmenting the volume of ventricle, especially in patients with AD (Kempton et al. 2011; Mayer et al. 2016).

Group-wise ventricular surface morphometry analysis

To better explore the morphological changes of ventricular surface, we extracted several vertex-wise characteristics consisting of radial distance (RD), tensor-based morphometry (TBM), multivariate TBM (mTBM), and RDMTBM (Zhang et al. 2016). The RD was defined as the shortest distance from each vertex to the medial axis (Thompson et al. 2004; Pizer et al. 1999), reflecting the morphological changes in thickness. Suppose φ: $S_1 \rightarrow S_2$ is a map from face S_1 to S_2. The derivative map $d\varphi$ is approximated by the linear map from one face $[v_1, v_2, v_3]$ to another face $[w_1, w_2, w_3]$. Then, the Jacobian matrix J is discrete derivative map $d\varphi$ from a face on anatomical surface to a face on the parameter domain, which can be computed as (Wang et al. 2009; Yao et al. 2020):

$$J = [w_3 - w_1, w_2 - w_1][v_3 - v_1, v_2 - v_1]^{-1}$$

The deformation tensor S is defined as $(J^T J)^{1/2}$. Instead of analyzing shape change based on the eigenvalues of the deformation tensor, MTBM considered "Log-Euclidean metrics" of deformation tensor S (Arsigny et al. 2006) so that the transformed values form a vector space. MTBM can be easily computed using the standard formulae for Euclidean spaces, and has increased the statistical power (Shi et al. 2013; Wang et al. 2010).

TBM was defined as $\sqrt{detJ}$, which reflected the changes in local surface area. MTBM was expressed as $\log\sqrt{JJ^T}$ and used to supplement the information of TBM. In addition, RDMTBM was a synthesis of RD and MTBM information, but more details of this feature still need to be further explored.

The human *ApoE* gene has three polymorphic alleles, named E2, E4, and E4. The E4 of *ApoE* is the major genetic risk factor for AD (Lyall et al. 2016; O'Donoghue et al. 2018), conversely, the E2 of *ApoE* has a protective effect against AD (Suri et al. 2013; Corder et al. 1994). After removing subjects carrying the *ApoE* E2E4 genotype, all subjects were divided into *ApoE* E4 carriers (E3E4, E4E4) and non-carriers (E2E3, E3E3). For the other genetic loci in this study, we assumed that minor allele frequencies from each SNP investigated were high-risk alleles. Due to the scarcity of homozygous for the minor allele, heterozygous and homozygous minor allele genotypes were combined as risk-allele carriers. We performed chi-squared test and two-sample t test on the risk-allele carriers and non-carriers based on each AD loci to analyze sex and age differences between the groups (As shown in eTable 1). In addition, two-sample t test was also used to analyze whether there is a significant difference in TIV between two groups. The vertex-based morphological differences between the two groups were compared by Hotelling's T^2 test and permutation test was used to correct the multiple comparisons (Hotelling 1992). First, we computed the Mahalanobis distance with true labels to quantify the difference between two groups on this vertex. Then, the surfaces were partitioned randomly into two groups with the same number of subjects in the true group and the Mahalanobis distance on each surface vertex was re-computed. This process was repeated for 10,000 times so that each vertex had 10,000 permutation values. The probability on each vertex was defined as ratio of the number of permutation values which were greater than the true group difference value. With these vertex-based probabilities (p values), we can generate a p-map with significant morphological changes (uncorrected, Fig. 2). The features will be compared with the features derived from the random groupings, thus, we can obtain a ratio that describes the fraction of the time an effect of similar or greater magnitude to the real effect occurs in the random assignments. This ratio reflects the global significance (corrected) of the p-map. Corrected P value < 0.05 was considered as significant.

In addition, to ensure an accurate reflection of the atrophy and expansion of each vertex, we used the following formula:

$$R^k = \frac{\sum_i^{N_1} F_{1i}^k}{N_1} - \frac{\sum_j^{N_2} F_{2j}^k}{N_2},$$

where F_{1i}^k and F_{2j}^k represent the feature of the i-th subject in group1 and j-th in group 2, such as RD, TBM, MTBM or RDMTBM. N_1 and N_2 are the number of group 1 and group 2, while k represents the k-th vertex on the surface. $R^k > 0$ indicates that the k-th vertex on the ventricular surfaces of

risk-allele carriers was expanding compared to the risk-allele non-carriers, while $R^k < 0$ indicates atrophy. There were 21,760 and 23,584 vertexes for the left and right lateral ventricles, respectively.

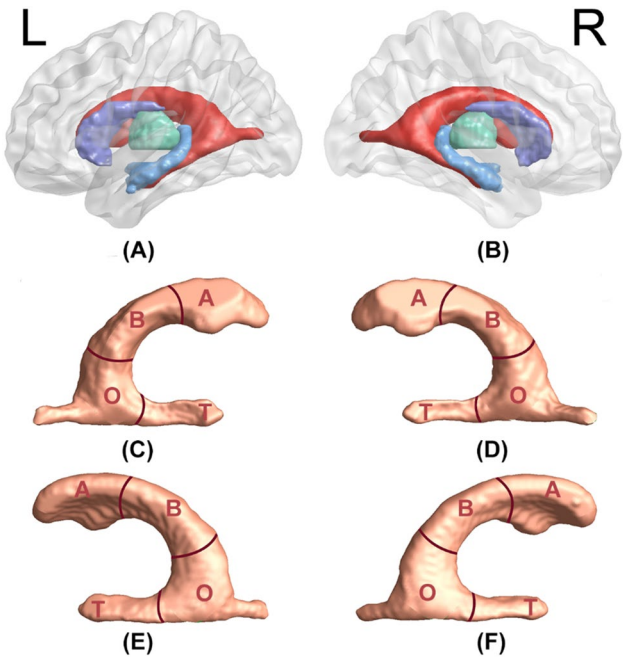

Fig. 1 The surrounding structure and subregions of lateral ventricle. **A**, **B** The subcortical structure around the lateral ventricle, including hippocampus (blue), thalamus (green), and caudate nucleus (purple). **C**–**F** The four subregions of lateral ventricle. *A* anterior horn, *B* body, *O* occipital horn, *T* temporal horn, *L* left, *R* right

Correlation analysis between morphological features and MoCA subscales

MoCA is a widely used screening tool to detect the cognitive impairment of clinical populations, including visuospatial, orientation, language, attention, abstraction, naming, and delayed recall (Folstein et al. 1975). To evaluate the functions of different subregions of lateral ventricle, Pearson correlation analyses were performed for the RD of each vertex and the sub-scores of all participants, and only significant correlations (false discovery rate, FDR < 0.05) were considered. The correlation analysis for each scale was done separately. The subregions and surrounding structure of lateral ventricle are shown in Fig. 1.

Results

Characteristics of subjects

The demographic characteristics of all subjects are shown in Table 2. The groupings based on each susceptibility loci were all gender- and age-matched ($p > 0.05$). There was also no significant difference between groups in TIV.

Impact of risk-allele on ventricular volume

A significantly decreased ventricular volume was found only in the C allele carriers at *BIN1* rs744373 loci when compared with non-carriers, especially left ventricle. The same trends (not significant) were obtained in the AD, MCI, and NC group, respectively (Table 3). For other loci, ventricular

Table 2 Demographic information of participants

	NC ($n=152$)	MCI ($n=239$)	AD ($n=19$)	Total ($n=410$)
Gender (F/M)	92/60	131/108	13/6	236/174
Age	74.08 ± 7.15	70.73 ± 7.11	74.65 ± 7.253	72.15 ± 7.15
LVV	$1.50\times10^4 \pm 7.75\times10^3$	$1.69\times10^4 \pm 1.02\times10^4$	$2.22\times10^4 \pm 9.25\times10^3$	$1.62\times10^4 \pm 9.45\times10^3$
RVV	$1.40\times10^4 \pm 6.79\times10^3$	$1.53\times10^4 \pm 9.23\times10^3$	$2.05\times10^4 \pm 7.63\times10^3$	$1.51\times10^4 \pm 8.42\times10^3$
TIV	$1.47\times10^6 \pm 1.47\times10^5$	$1.49\times10^6 \pm 1.98\times10^5$	$1.43\times10^6 \pm 1.58\times10^5$	$1.48\times10^6 \pm 1.79\times10^5$
MoCA	24.42 ± 4.32	21.94 ± 4.31	16.05 ± 4.41	22.59 ± 4.30
Visuospatial	4.17 ± 0.92	3.62 ± 1.37	2.21 ± 1.40	3.76 ± 1.30
Naming	2.82 ± 0.47	2.69 ± 0.68	2.31 ± 0.89	2.72 ± 0.63
Attention	4.88 ± 0.89	4.28 ± 1.29	3.15 ± 1.34	4.45 ± 1.22
Language	2.35 ± 0.80	2.20 ± 0.90	1.00 ± 1.15	2.20 ± 0.92
Abstraction	1.79 ± 0.46	1.62 ± 0.64	0.84 ± 0.90	1.64 ± 0.62
Delayed recall	1.84 ± 1.78	1.22 ± 1.64	0.16 ± 0.69	1.40 ± 1.71
Orientation	5.71 ± 0.83	5.00 ± 1.66	2.53 ± 1.84	5.15 ± 1.56

$\pm$: standard deviation

F female; *M* male; *NC* normal controls; *MCI* mild cognitive impairment; *AD* Alzheimer's disease; *MoCA* Montreal Cognitive Assessment; *LVV* left lateral ventricular volume; *RVV* right lateral ventricular volume; *TIV* total intracranial volume

Table 3 Differences of ventricular volume at the *BIN1* rs744373 loci

BIN1	TT ($n=182$)	CT+CC ($n=197$)	P value
Age	72.53 ± 7.38	72.11 ± 6.9300	0.57
Gender (F/M)	105/77	112/85	0.87
LVV (Total)	$1.77\times10^4 \pm 1.06\times10^4$	$1.55\times10^4 \pm 8.38\times10^3$	**0.02**
RVV (Total)	$1.60\times10^4 \pm 9.00\times10^3$	$1.43\times10^4 \pm 7.85\times10^3$	**0.04**
LVV (AD)	$2.31\times10^4 \pm 9.76\times10^4$	$2.01\times10^4 \pm 7.02\times10^3$	0.49
RVV (AD)	$2.07\times10^4 \pm 7.53\times10^3$	$1.93\times10^4 \pm 5.63\times10^3$	0.68
LVV (MCI)	$1.83\times10^4 \pm 1.12\times10^4$	$1.62\times10^4 \pm 9.49\times10^3$	0.13
RVV (MCI)	$1.63\times10^4 \pm 1.00\times10^4$	$1.48\times10^4 \pm 8.66\times10^3$	0.24
LVV (NC)	$1.61\times10^4 \pm 9.20\times10^3$	$1.40\times10^4 \pm 6.41\times10^3$	0.09
RVV (NC)	$1.50\times10^4 \pm 7.06\times10^3$	$1.30\times10^4 \pm 6.52\times10^3$	0.07
TIV	$1.49\times10^6 \pm 1.96\times10^5$	$1.48\times10^6 \pm 1.62\times10^5$	0.51

Bold values indicate significant difference between the two groups (p value < 0.05)

$\pm$: standard deviation

F female; *M* male; *LVV* left lateral ventricular volume; *RVV* right lateral ventricular volume; *TIV* total intracranial volume

volume had a decreasing or increasing trend, but did not reach the significant level (Fig. 2).

Ventricular morphometric differences between risk-allele carriers and non-carriers

To achieve a better understanding of the morphological changes of lateral ventricle, we analyzed the surface differences using the vertex-wise characteristics. The p-map of *BIN1* rs744373 genotype on ventricular surface is shown in Fig. 3, which reflected the areas of significant abnormality caused by risk allele. Consistent with the results of volume, ventricular surface subregions of C allele carriers showed significant atrophy. As for the RD and TBM, the atrophy was mainly in the dorsolateral anterior horn and body of left lateral ventricle, with a few areas in occipital horn, and the difference in TBM was greater than RD (Fig. 3A,B). Other than that, the abnormal changes of mTBM/RDmTBM were concentrated on the temporal horn, dorsolateral of anterior horn, and a few areas in occipital horn (Fig. 3C, D).

Although trends of morphological changes are observed in other genetic loci, they did not pass the correction (overall p value > 0.05), including *CD33* rs3865444, *CLU* rs7012010, *PICALM* rs3851179, *CD2AP* rs9296562, and *PTK2B* rs1879189. The results of this part of the study were not described here because they did not reach statistical significance.

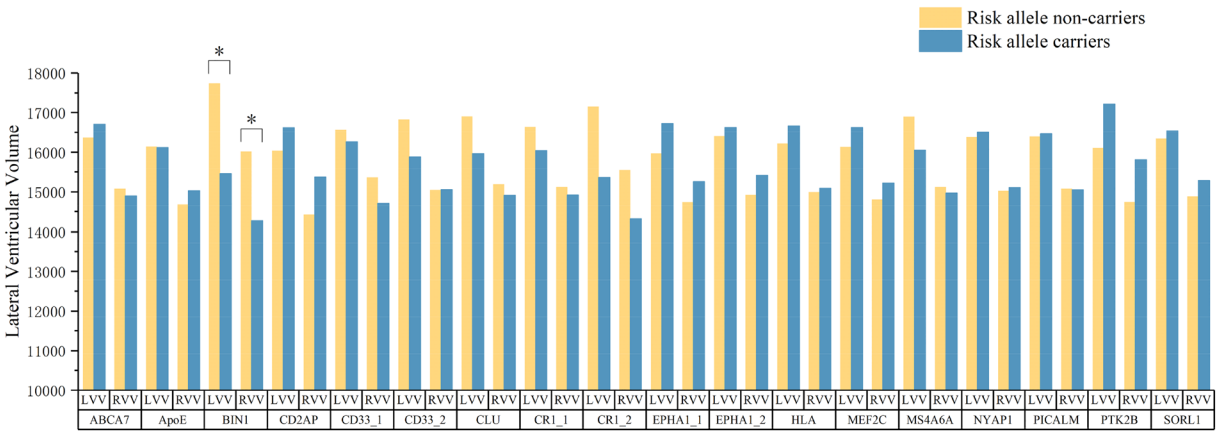

Fig. 2 The mean lateral ventricular volume of each group. *RVV* right lateral ventricular volume; *LVV* left lateral ventricular volume; *CD33_1: CD33*(rs3865444); *CD33_2: CD33*(rs11771145); *CR1_1: CR1*(rs3818361); *CR1_2: CR1*(rs6691117); *EPHA1_1: EPHA1*(rs11771145); *EPHA1_2: EPHA1*(rs11767557). *Means significant difference between risk-allele carriers and non-carriers

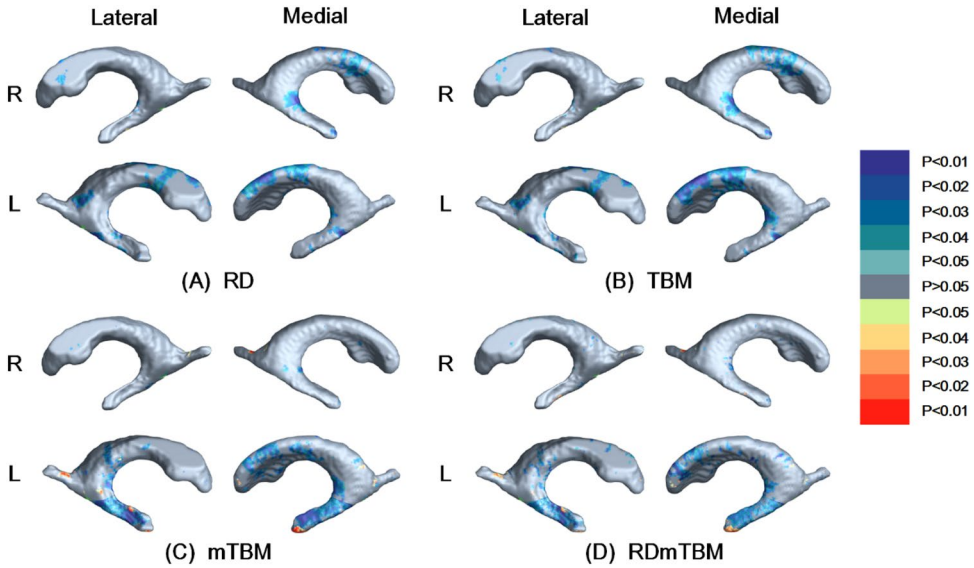

Fig. 3 P-map of *BIN1* rs744373 genotype on lateral ventricular surface. The overall corrected *p* values of right ventricular were all > 0.05, and the overall corrected *p* values of RD, TBM, mTBM, and RDmTBM of left ventricular were 0.0546, 0.0283, 0.0087, and 0.0113, indicating significant changes in left lateral ventricle. The warm and cool color each represents the expansion (risk-allele carriers > risk-allele non-carriers) and atrophy (risk-allele carriers < risk-allele non-carriers) of ventricular surfaces. *L* left; *R* right

Correlation between surface features of lateral ventricular subregions and cognitive subscales

The higher MoCA scores, the higher cognitive functional performance. After the correlation analysis, significant negative correlation between delayed recall score and RD was observed in most areas of bilateral ventricular surface (Fig. 4A). Results showed that language scores were significantly negative correlated with RD in the right temporal horn, as well as visuospatial scores in trigone area of the left lateral ventricle (Fig. 4B, D). Apart from this, A significant negative correlation was found between the orientation scores and morphological feature of body, occipital horn, and temporal horn of left lateral ventricle (Fig. 4C). For the total score of MoCA, significant negative correlations were found in body, occipital horn, and temporal horn of bilateral lateral ventricle (Fig. 4E). RD showed no significantly correlated with attention, abstraction, and naming scores.

Discussion

We evaluated the association between 18 AD susceptibility loci and surface morphology of the lateral ventricle. The surrounding parenchymal areas that can be involved in cognition functions were firstly reported in our research. Our

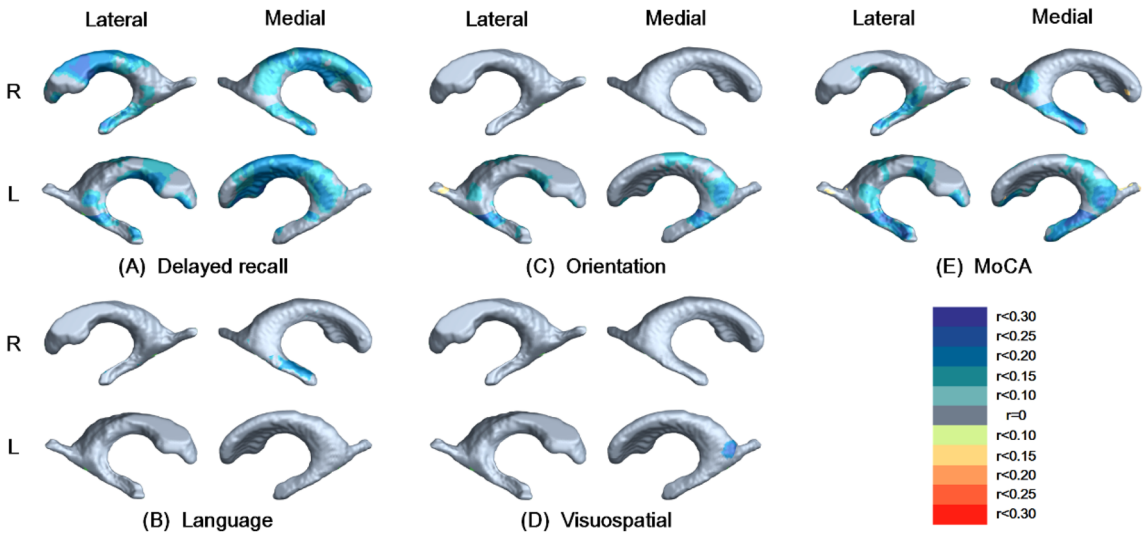

Fig. 4 Correlations between ventricular surface morphological feature and MoCA, subscales, respectively (FDR < 0.05). Warm colors represent positive correlations and cool colors represent negative correlations. *MoCA* Montreal Cognitive Assessment; *L* left; *R* right

results showed that only the lateral ventricular morphology of C allele carriers at *BIN1* rs744373 loci were significantly different from non-carriers, as well as the cognitive scales were significantly associated with ventricular surface metric. The current findings provided important evidence for the limited effects of AD risk genes on the lateral ventricle.

Consistent with previous study(Nestor et al. 2008), our results showed that AD patients had the largest ventricular volume, followed by MCI and then for NC (Table 2), which reflected that lateral ventricle had a progressive expansion of volume with the development of AD. Risk genes were related to the increased AD incidence and could cause abnormal expansion of ventricle in the elderly (Karch and Goate 2015; Roussotte et al. 2014b; Erten-Lyons et al. 2013), which was mainly due to the atrophy of the subcortical structures around the lateral ventricles, including hippocampal (Stoub et al. 2010), thalamus (Zarei et al. 2010), and caudate nucleus (Madsen et al. 2010), etc. Nevertheless, the atrophy of ventricular surface was observed in C allele carriers at the SNP rs744373.

Lateral ventricle is adjacent to several AD-related brain structures, including hippocampus, thalamus, caudate nucleus, and corpus callosum (Fig. 1), thus, ventricle and surrounding structures have an ability to influence each other reciprocally(Tang et al. 2014; Shi et al. 2015). In contrast to the *ApoE* and *CLU* rs11136000, carriers of the C risk allele at rs744373 showed significant atrophy in temporal horn and dorsolateral of anterior horn/body (Fig. 3), as well as the volume of C allele carriers was significantly reduced (Table 3), which implying that the surrounding subcortical structures had not yet significantly atrophy. It is well known that some known AD risk allele (*ApoE* E4, C allele at *CLU* rs11136000, etc.) accelerate the atrophy of AD-related biomarker and cognitive decline (Roussotte et al. 2014b; An et al. 2021). Therefore, the atrophy of lateral ventricle may reflect the protective role of this locus for brain atrophy. The temporal horn locates in the dorsolateral area of hippocampus, and prior research had found that healthy homozygous carriers of the risk allele at rs744373 showed significantly increased gray matter volume (GMV) in the bilateral temporal cortex, including hippocampus, amygdala, and parahippocampal gyrus (Zhang et al. 2015). Genetic factors could affect white matter density of the corpus callosum (Pol et al. 2006), which was above the dorsolateral of anterior horn, body, and occipital horn (Karakaş et al. 2011), so perhaps C allele at rs744373 suppress the atrophy of the bottom of corpus callosum. The most likely explanation for the decreased lateral ventricular volume was the compensatory recruitment of neural resources, which could help AD patients to maintain a certain level of cognitive performance (Buckner 2004). Increased recruitment is a compensatory response to maintain cognitive function. Brain atrophy and cognitive decline in AD patients are undoubtedly an intricate process, including vascular compromise, amyloid deposits, neuron loss, and neurotransmitter depletion (Buckner 2004), etc. *BIN1* is located on chromosome 2q, has been identified as the second most important locus for AD, after *ApoE* (Tan et al. 2013). It also plays a role in the regulation of tau pathology, amyloid-β peptide (Aβ), apoptosis, and cytoskeleton integrity (Franzmeier et al. 2019), The levels of tau and Aβ were all reported to be related to the ventricular volume (Ott et al. 2010). Meanwhile, one study mentioned *BIN1* has a specific role in postsynaptic sites in the brain, leading to an increase in pCaMKII cluster volume as a compensatory response to presynaptic changes (De Rossi et al. 2020).

ApoE, BIN1, CLU, PICALM, and *CR1* were five most widely studied AD susceptibility loci in neuroimaging. For the association between susceptibility loci and ventricular surface morphology, except for *BIN1* rs744373, other loci did not pass the correction in our study (Fig. 2). However, this does not necessarily indicate that other susceptibility loci have no effect on the changes in lateral ventricle, perhaps due to the cross-sectional data and the insufficient statistical power to detect subtle differences in surface. In particular, the number of minor allele homozygous subjects was relatively small. The enlargement of lateral ventricle volume is known to be a consequence of multiple risk factors rather than a single cause, such as dietary cholesterol (Schreurs et al. 2013) and systemic inflammation (Walker et al. 2017).

MoCA total score reflects the cognitive profiles of participant (Freitas et al. 2012). The cognitive function was primarily associated with the bilateral occipital horns (Fig. 4E) adjacent to the hippocampus, which is the most affected structure of brain in AD patients (den Heijer et al. 2010). Impaired memory is a typical symptom of AD. Our results suggested that delayed recall function was associated with the whole lateral ventricle, particularly in anterior horn and body (Fig. 4A), which was an indirect proof of the relationship between memory and hippocampus, thalamus, caudate, corpus callosum, respectively(Preston and Eichenbaum 2013; O'Mara 2013; Stoffers et al. 2014; Qiu et al. 2016). In term of the language function, only the temporal horn of right ventricle exhibited significant correlation (Fig. 4B). In addition, for visuospatial function, the trigone area of the left lateral ventricle showed a strong association (Fig. 4D), adjacent to the motor and sensory centers in the parietal lobe (Ma et al. 2014a). Smaller areas of body, occipital horn and temporal horn of left lateral ventricle were related to the orientation function (Fig. 4C). Apart from delayed recall, AD patients also showed variable degrees of impairments in language, visuospatial, and orientation domains (Cloutier et al. 2015). These results may further prove that surrounding structures were crucial for cognitive function.

The current study had several potential limitations. First, and as stated, this study was cross-sectional, which could not evaluate the long-term impact of risk allele. Previous

related studies of *ApoE* and *CLU* observed significant effects on lateral ventricular surface morphology at the 24-month follow-up (Roussotte et al. 2014a, b), so the longitudinal study may reveal the effects of other loci. Second, we could not determine if the effect of these genes were additive or interactive. Our study focused on the single variant, while ignoring the complex interactions between genes. Third, previous studies have mentioned that there is no significant correlation between head movement and voxel-based morphology, subcortical structures segmentation, respectively (Cole et al. 2017; Pardoe et al. 2016), but we think it is necessary to introduce accurately measured head motion parameters into the analysis process. We did not consider the subject motion in our analysis due to a lack of data on level of motion. Finally, the relatively small sample size may restrict the generalizability of the results. Our conclusion should be validated in other larger databases, such as UK Biobank (Sudlow et al. 2015), ENIGMA (Thompson et al. 2014) and NDAR (Hall et al. 2012).

In conclusion, our present study revealed that in the 18 AD susceptibility loci, only *BIN1* rs744373 had a significant impact on the ventricular surface. There is not always a direct relationship between genes and brain changes, but was conducted by multiple risk factors with complex mechanism. In addition, we found that different subregions of lateral ventricle were related to various cognitive functions, including delayed recall, orientation, language, and visuospatial. The current finding provided evidence for the underlying mechanisms of *BIN1*, and altered surface morphology of lateral ventricle contributed to the study about the surrounding brain structures to search for the reliable biomarkers of AD.

Supplementary Information The online version contains supplementary material available at https://doi.org/10.1007/s00429-021-02429-y.

Acknowledgements This work was supported in part by the National Key Research and Development Program of China (Grant No. 2019YFA0706200), in part by the National Natural Science Foundation of China (Grant No.61632014, No.61627808), in part by the Fundamental Research Funds for the Central Universities(lzuxxxy-2019-tm09), in part by the Natural Science Foundation of Gansu Province of China (Grant No.20JR5RA292), and in part by the Department of Education of Gansu Province: "Innovation Star" Project for Excellent Postgraduates (2021CXZX-121).

Author contributions SL: conceptualization, formal analysis, and writing—original draft. NA: methodology and visualization. NC: formal analysis and visualization. YW: writing—original draft and investigation. LY: writing—original draft and investigation. YW: methodology. ZY: conceptualization and supervision. BH: conceptualization and supervision.

Funding Data collection and sharing for this project was funded by the Alzheimer's Disease Neuroimaging Initiative (ADNI) (National Institutes of Health Grant U01 AG024904) and DOD ADNI (Department of Defense award number W81XWH-12-2-0012). ADNI is funded by the National Institute on Aging, the National Institute of Biomedical Imaging and Bioengineering, and through generous contributions from the following: AbbVie, Alzheimer's Association; Alzheimer's Drug Discovery Foundation; Araclon Biotech; BioClinica, Inc.; Biogen; Bristol-Myers Squibb Company; CereSpir, Inc.; Cogstate; Eisai Inc.; Elan Pharmaceuticals, Inc.; Eli Lilly and Company; EuroImmun; F. Hoffmann-La Roche Ltd and its affiliated company Genentech, Inc.; Fujirebio; GE Healthcare; IXICO Ltd.; Janssen Alzheimer Immunotherapy Research & Development, LLC.; Johnson & Johnson Pharmaceutical Research & Development LLC.; Lumosity; Lundbeck; Merck & Co., Inc.; Meso Scale Diagnostics, LLC.; NeuroRx Research; Neurotrack Technologies; Novartis Pharmaceuticals Corporation; Pfizer Inc.; Piramal Imaging; Servier; Takeda Pharmaceutical Company; and Transition Therapeutics. The Canadian Institutes of Health Research is providing funds to support ADNI clinical sites in Canada. Private sector contributions are facilitated by the Foundation for the National Institutes of Health (www.fnih.org). The grantee organization is the Northern California Institute for Research and Education, and the study is coordinated by the Alzheimer's Therapeutic Research Institute at the University of Southern California. ADNI data are disseminated by the Laboratory for Neuro Imaging at the University of Southern California.

Availability of data and material All data used are from the Alzheimer's Disease Neuroimaging Initiative (ADNI) database (adni.loni.usc.edu).

Code availability The code we used can be obtained by contacting the corresponding authors.

Declarations

Conflict of interest There is no conflict of interest to disclose.

Ethics approval Data involved in the study came from the publicly open Alzheimer's disease neuroimaging initiative (ADNI) database. All procedures performed in studies involving human participants were in accordance with the ethical standards of the institutional and/or national research committee and with the Helsinki Declaration of 1975.

References

Alimajstorovic Z, Pascual-Baixauli E, Hawkes CA, Sharrack B, Loughlin AJ, Romero IA, Preston JE (2020) Cerebrospinal fluid dynamics modulation by diet and cytokines in rats. Fluids Barriers CNS 17(1):10

An N, Fu Y, Shi J, Guo H-N, Yang Z-W, Li Y-C, Li S, Wang Y, Yao Z-J, Hu B (2021) Synergistic effects of APOE and CLU may increase the risk of alzheimer's disease: acceleration of atrophy in the volumes and shapes of the hippocampus and amygdala. J Alzheimer Dis 80(3):1311–1327. https://doi.org/10.3233/JAD-201162

Apostolova LG, Green AE, Babakchanian S, Hwang KS, Chou Y-Y, Toga AW, Thompson PM (2012) Hippocampal atrophy and ventricular enlargement in normal aging, mild cognitive impairment and Alzheimer's disease. Alzheimer Dis Assoc Disord 26(1):17. https://doi.org/10.1097/WAD.0b013e3182163b62

Arsigny V, Fillard P, Pennec X, Ayache N (2006) Log-Euclidean metrics for fast and simple calculus on diffusion tensors. Magn Reson Med 56(2):411–421. https://doi.org/10.1002/mrm.20965

As A (2019) 2019 Alzheimer's disease facts and figures. Alzheimers Dement 15(3):321–387

Ashburner J, Friston KJ (2011) Diffeomorphic registration using geodesic shooting and Gauss-Newton optimisation. Neuroimage 55(3):954–967. https://doi.org/10.1016/j.neuroimage.2010.12.049

Bae I-S, Kim JM, Cheong JH, Ryu JI, Han M-H (2019) Association between bone mineral density and brain parenchymal atrophy and ventricular enlargement in healthy individuals. Aging (albany N Y) 11(19):8217. https://doi.org/10.18632/aging.102316

Barami K, Sloan AE, Rojiani A, Schell MJ, Staller A, Brem S (2009) Relationship of gliomas to the ventricular walls. J Clin Neurosci 16(2):195–201. https://doi.org/10.1016/j.jocn.2008.03.006

Beecham GW, Martin ER, Li Y-J, Slifer MA, Gilbert JR, Haines JL, Pericak-Vance MA (2009) Genome-wide association study implicates a chromosome 12 risk locus for late-onset Alzheimer disease. Am J Hum Genet 84(1):35–43. https://doi.org/10.1016/j.ajhg.2008.12.008

Bertram L, Lange C, Mullin K, Parkinson M, Hsiao M, Hogan MF, Schjeide BM, Hooli B, DiVito J, Ionita I (2008) Genome-wide association analysis reveals putative Alzheimer's disease susceptibility loci in addition to APOE. Am J Hum Genet 83(5):623–632. https://doi.org/10.1016/j.ajhg.2008.10.008

Buckner RL (2004) Memory and executive function in aging and AD: multiple factors that cause decline and reserve factors that compensate. Neuron 44(1):195–208. https://doi.org/10.1016/j.neuron.2004.09.006

Chauhan G, Adams HH, Bis JC, Weinstein G, Yu L, Töglhofer AM, Smith AV, Van Der Lee SJ, Gottesman RF, Thomson R (2015) Association of Alzheimer's disease GWAS loci with MRI markers of brain aging. Neurobiol Aging 36(4):1765.e7-1765.e16. https://doi.org/10.1016/j.neurobiolaging.2014.12.028

Cloutier S, Chertkow H, Kergoat M-J, Gauthier S, Belleville S (2015) Patterns of cognitive decline prior to dementia in persons with mild cognitive impairment. J Alzheimers Dis 47(4):901–913. https://doi.org/10.3233/JAD-142910

Cole JH, Poudel RP, Tsagkrasoulis D, Caan MW, Steves C, Spector TD, Montana G (2017) Predicting brain age with deep learning from raw imaging data results in a reliable and heritable biomarker. Neuroimage 163:115–124

Corder E, Saunders AM, Risch N, Strittmatter W, Schmechel D, Gaskell P, Rimmler J, Locke P, Conneally P, Schmader K (1994) Protective effect of apolipoprotein E type 2 allele for late onset Alzheimer disease. Nat Genet 7(2):180–184

Crivello F, Lemaître H, Dufouil C, Grassiot B, Delcroix N, Tzourio-Mazoyer N, Tzourio C, Mazoyer B (2010) Effects of ApoE-ε4 allele load and age on the rates of grey matter and hippocampal volumes loss in a longitudinal cohort of 1186 healthy elderly persons. Neuroimage 53(3):1064–1069. https://doi.org/10.1016/j.neuroimage.2009.12.116

Dadar M, Fonov VS, Collins DL, AsDN I (2018) A comparison of publicly available linear MRI stereotaxic registration techniques. Neuroimage 174:191–200

de Leon MJ, George AE, Reisberg B, Ferris SH, Kluger A, Stylopoulos LA, Miller JD, La Regina ME, Chen C, Cohen J (1989) Alzheimer's disease: longitudinal CT studies of ventricular change. Am J Roentgenol 152(6):1257–1262. https://doi.org/10.2214/ajr.152.6.1257

De Rossi P, Nomura T, Andrew RJ, Masse NY, Sampathkumar V, Musial TF, Sudwarts A, Recupero AJ, Le Metayer T, Hansen MT (2020) Neuronal BIN1 regulates presynaptic neurotransmitter release and memory consolidation. Cell Rep 30(10):3520-3535.e7

den Heijer T, van der Lijn F, Koudstaal PJ, Hofman A, van der Lugt A, Krestin GP, Niessen WJ, Breteler MM (2010) A 10-year follow-up of hippocampal volume on magnetic resonance imaging in early dementia and cognitive decline. Brain 133(4):1163–1172

Dong Q, Zhang W, Stonnington CM, Wu J, Gutman BA, Chen K, Su Y, Baxter LC, Thompson PM, Reiman EM (2020) Applying surface-based morphometry to study ventricular abnormalities of cognitively unimpaired subjects prior to clinically significant memory decline. NeuroImage-Clin. https://doi.org/10.1016/j.nicl.2020.102338

Erten-Lyons D, Dodge HH, Woltjer R, Silbert LC, Howieson DB, Kramer P, Kaye JA (2013) Neuropathologic basis of age-associated brain atrophy. JAMA Neurol 70(5):616–622

Ewers M, Walsh C, Trojanowski JQ, Shaw LM, Petersen RC, Jack CR Jr, Feldman HH, Bokde AL, Alexander GE, Scheltens P (2012) Prediction of conversion from mild cognitive impairment to Alzheimer's disease dementia based upon biomarkers and neuropsychological test performance. Neurobiol Aging 33(7):1203-1214.e2. https://doi.org/10.1016/j.neurobiolaging.2010.10.019

Folstein MF, Folstein SE, McHugh PR (1975) "Mini-mental state": a practical method for grading the cognitive state of patients for the clinician. J Psychiatr Res 12(3):189–198

Franzmeier N, Rubinski A, Neitzel J, Ewers M (2019) The BIN1 rs744373 SNP is associated with increased tau-PET levels and impaired memory. Nat Commun 10(1):1–12. https://doi.org/10.1038/s41467-019-09564-5

Freitas S, Simões MR, Alves L, Duro D, Santana I (2012) Montreal Cognitive Assessment (MoCA): validation study for frontotemporal dementia. J Geriatr Psychiatry Neurol 25(3):146–154

Frisoni GB, Pievani M, Testa C, Sabattoli F, Bresciani L, Bonetti M, Beltramello A, Hayashi KM, Toga AW, Thompson PM (2007) The topography of grey matter involvement in early and late onset Alzheimer's disease. Brain 130(3):720–730. https://doi.org/10.1093/brain/awl377

Grasby KL, Jahanshad N, Painter JN, Colodro-Conde L, Bralten J, Hibar DP, Lind PA, Pizzagalli F, Ching CR, McMahon MAB (2020) The genetic architecture of the human cerebral cortex. Science 367(6484):eaay6690

Guo M, Li Y, Zheng W, Huang K, Zhou L, Hu X, Yao Z, Hu B (2020) A novel conversion prediction method of MCI to AD based on longitudinal dynamic morphological features using ADNI structural MRIs. J Neurol. https://doi.org/10.1007/s00415-020-09890-5

Gutman BA, Hua X, Rajagopalan P, Chou Y-Y, Wang Y, Yanovsky I, Toga AW, Jack CR Jr, Weiner MW, Thompson PM (2013) Maximizing power to track Alzheimer's disease and MCI progression by LDA-based weighting of longitudinal ventricular surface features. Neuroimage 70:386–401

Hall D, Huerta MF, McAuliffe MJ, Farber GK (2012) Sharing heterogeneous data: the national database for autism research. Neuroinformatics 10(4):331–339

Hofer E, Roshchupkin GV, Adams HH, Knol MJ, Lin H, Li S, Zare H, Ahmad S, Armstrong NJ, Satizabal CL (2020) Genetic correlations and genome-wide associations of cortical structure in general population samples of 22,824 adults. Nat Commun 11(1):1–16

Hotelling H (1992) The generalization of Student's ratio. Breakthroughs in statistics. Springer, pp 54–65. https://doi.org/10.1007/978-1-4612-0919-5_4

Jack CR Jr, Bernstein MA, Fox NC, Thompson P, Alexander G, Harvey D, Borowski B, Britson PJ, Whitwell JL, Ward C (2008) The Alzheimer's disease neuroimaging initiative (ADNI): MRI methods. J Magn Reson Imaging 27(4):685–691. https://doi.org/10.1002/jmri.21049

Jovicich J, Marizzoni M, Sala-Llonch R, Bosch B, Bartrés-Faz D, Arnold J, Benninghoff J, Wiltfang J, Roccatagliata L, Nobili F (2013) Brain morphometry reproducibility in multi-center 3 T MRI studies: a comparison of cross-sectional and longitudinal segmentations. Neuroimage 83:472–484. https://doi.org/10.1016/j.neuroimage.2013.05.007

Karakaş P, Koç Z, Koç F, Gülhal Bozkır M (2011) Morphometric MRI evaluation of corpus callosum and ventricles in normal adults. Neurol Res 33(10):1044–1049

Karch CM, Goate AM (2015) Alzheimer's disease risk genes and mechanisms of disease pathogenesis. Biol Psychiatry 77(1):43–51. https://doi.org/10.1016/j.biopsych.2014.05.006

Kempton MJ, Underwood TS, Brunton S, Stylios F, Schmechtig A, Ettinger U, Smith MS, Lovestone S, Crum WR, Frangou S (2011) A comprehensive testing protocol for MRI neuroanatomical segmentation techniques: evaluation of a novel lateral ventricle segmentation method. Neuroimage 58(4):1051–1059. https://doi.org/10.1016/j.neuroimage.2011.06.080

Kunkle BW, Grenier-Boley B, Sims R, Bis JC, Damotte V, Naj AC, Boland A, Vronskaya M, Van Der Lee SJ, Amlie-Wolf A (2019) Genetic meta-analysis of diagnosed Alzheimer's disease identifies new risk loci and implicates Aβ, tau, immunity and lipid processing. Nat Genet 51(3):414–430

Lambert J-C, Ibrahim-Verbaas CA, Harold D, Naj AC, Sims R, Bellenguez C, Jun G, DeStefano AL, Bis JC, Beecham GW (2013) Meta-analysis of 74,046 individuals identifies 11 new susceptibility loci for Alzheimer's disease. Nat Genet 45(12):1452–1458. https://doi.org/10.1038/ng.2802

Li B, Shi J, Gutman BA, Baxter LC, Thompson PM, Caselli RJ, Wang Y, AsDN I (2016) Influence of APOE genotype on hippocampal atrophy over time-an N= 1925 surface-based ADNI study. PLoS One 11(4):e0152901. https://doi.org/10.1371/journal.pone.0152901

Li J-Q, Wang H-F, Zhu X-C, Sun F-R, Tan M-S, Tan C-C, Jiang T, Tan L, Yu J-T, AsDN I (2017) GWAS-linked loci and neuroimaging measures in Alzheimer's disease. Mol Neurobiol 54(1):146–153. https://doi.org/10.1007/s12035-015-9669-1

Liu G, Sun J-Y, Xu M, Yang X-Y, Sun B-L (2017) SORL1 variants show different association with early-onset and late-onset Alzheimer's disease risk. J Alzheimers Dis 58(4):1121–1128. https://doi.org/10.3233/JAD-170005

Lyall DM, Ward J, Ritchie SJ, Davies G, Cullen B, Celis C, Bailey ME, Anderson J, Evans J, Mckay DF (2016) Alzheimer disease genetic risk factor APOE e4 and cognitive abilities in 111,739 UK Biobank participants. Age Ageing 45(4):511–517

Ma J, Cheng L, Wang G, Lin S (2014a) Surgical management of meningioma of the trigone area of the lateral ventricle. World Neurosurg 82(5):757–769. https://doi.org/10.1016/j.wneu.2014.05.026

Ma X-Y, Yu J-T, Tan M-S, Sun F-R, Miao D, Tan L (2014b) Missense variants in CR1 are associated with increased risk of Alzheimer'disease in Han Chinese. Neurobiol Aging 35(2):443.e17-443.e21. https://doi.org/10.1016/j.neurobiolaging.2013.08.009

Madsen SK, Ho AJ, Hua X, Saharan PS, Toga AW, Jack CR Jr, Weiner MW, Thompson PM, AsDN I (2010) 3D maps localize caudate nucleus atrophy in 400 Alzheimer's disease, mild cognitive impairment, and healthy elderly subjects. Neurobiol Aging 31(8):1312–1325

Mayer KN, Latal B, Knirsch W, Scheer I, Von Rhein M, Reich B, Bauer J, Gummel K, Roberts N, Tuura ROG (2016) Comparison of automated brain volumetry methods with stereology in children aged 2 to 3 years. Neuroradiology 58(9):901–910

Nestor SM, Rupsingh R, Borrie M, Smith M, Accomazzi V, Wells JL, Fogarty J, Bartha R, AsDN I (2008) Ventricular enlargement as a possible measure of Alzheimer's disease progression validated using the Alzheimer's disease neuroimaging initiative database. Brain 131(9):2443–2454. https://doi.org/10.1093/brain/awn146

O'Mara SM (2013) The anterior thalamus provides a subcortical circuit supporting memory and spatial navigation. Front Syst Neurosci 7:45. https://doi.org/10.3389/fnsys.2013.00045

O'Donoghue MC, Murphy SE, Zamboni G, Nobre AC, Mackay CE (2018) APOE genotype and cognition in healthy individuals at risk of Alzheimer's disease: a review. Cortex 104:103–123

Ott BR, Cohen RA, Gongvatana A, Okonkwo OC, Johanson CE, Stopa EG, Donahue JE, Silverberg GD (2010) Brain ventricular volume and cerebrospinal fluid biomarkers of Alzheimer's disease. J Alzheimers Dis 20(2):647–657. https://doi.org/10.3233/JAD-2010-1406

Pardoe HR, Hiess RK, Kuzniecky R (2016) Motion and morphometry in clinical and nonclinical populations. Neuroimage 135:177–185

Pizer SM, Fritsch DS, Yushkevich PA, Johnson VE, Chaney EL (1999) Segmentation, registration, and measurement of shape variation via image object shape. IEEE Trans Med Imaging 18(10):851–865

Pol HEH, Schnack HG, Posthuma D, Mandl RC, Baaré WF, van Oel C, van Haren NE, Collins DL, Evans AC, Amunts K (2006) Genetic contributions to human brain morphology and intelligence. J Neurosci 26(40):10235–10242. https://doi.org/10.1523/JNEUROSCI.1312-06.2006

Poulin SP, Dautoff R, Morris JC, Barrett LF, Dickerson BC, AsDN I (2011) Amygdala atrophy is prominent in early Alzheimer's disease and relates to symptom severity. Psychiatry Res 194(1):7–13. https://doi.org/10.1016/j.pscychresns.2011.06.014

Preston AR, Eichenbaum H (2013) Interplay of hippocampus and prefrontal cortex in memory. Curr Biol 23(17):R764–R773

Purcell S, Neale B, Todd-Brown K, Thomas L, Ferreira MA, Bender D, Maller J, Sklar P, De Bakker PI, Daly MJ (2007) PLINK: a tool set for whole-genome association and population-based linkage analyses. Am J Hum Genet 81(3):559–575

Qiu Y, Liu S, Hilal S, Loke YM, Ikram MK, Xu X, Tan BY, Venketasubramanian N, Chen CL-H, Zhou J (2016) Inter-hemispheric functional dysconnectivity mediates the association of corpus callosum degeneration with memory impairment in AD and amnestic MCI. Sci Rep 6:32573. https://doi.org/10.1038/srep32573

Rhoton AL Jr (2002) The lateral and third ventricles. Neurosurgery 51(suppl_4):S1-207-S201-271. https://doi.org/10.1097/00006123-200210001-00006

Roussotte FF, Gutman BA, Madsen SK, Colby JB, Narr KL, Thompson PM, AsDN I (2014a) The apolipoprotein E epsilon 4 allele is associated with ventricular expansion rate and surface morphology in dementia and normal aging. Neurobiol Aging 35(6):1309–1317. https://doi.org/10.1016/j.neurobiolaging.2013.11.030

Roussotte FF, Gutman BA, Madsen SK, Colby JB, Thompson PM, AsDN I (2014b) Combined effects of Alzheimer risk variants in the CLU and ApoE genes on ventricular expansion patterns in the elderly. J Neurosci 34(19):6537–6545. https://doi.org/10.1523/JNEUROSCI.5236-13.2014

Saykin AJ, Shen L, Foroud TM, Potkin SG, Swaminathan S, Kim S, Risacher SL, Nho K, Huentelman MJ, Craig DW (2010) Alzheimer's Disease Neuroimaging Initiative biomarkers as quantitative phenotypes: genetics core aims, progress, and plans. Alzheimers Dement 6(3):265–273

Schreurs BG, Smith-Bell CA, Lemieux SK (2013) Dietary cholesterol increases ventricular volume and narrows cerebrovascular diameter in a rabbit model of Alzheimer's disease. Neuroscience 254:61–69. https://doi.org/10.1016/j.neuroscience.2013.09.015

Shah H, Albanese E, Duggan C, Rudan I, Langa KM, Carrillo MC, Chan KY, Joanette Y, Prince M, Rossor M (2016) Research priorities to reduce the global burden of dementia by 2025. Lancet Neurol 15(12):1285–1294. https://doi.org/10.1016/S1474-4422(16)30235-6

Shi J, Stonnington CM, Thompson PM, Chen K, Gutman B, Reschke C, Baxter LC, Reiman EM, Caselli RJ, Wang Y (2015) Studying ventricular abnormalities in mild cognitive impairment with hyperbolic Ricci flow and tensor-based morphometry. Neuroimage 104:1–20. https://doi.org/10.1016/j.neuroimage.2014.09.062

Shi J, Wang Y, Ceschin R, An X, Lao Y, Vanderbilt D, Nelson MD, Thompson PM, Panigrahy A, Leporé N (2013) A multivariate surface-based analysis of the putamen in premature newborns: regional differences within the ventral striatum. PLoS One 8(7):e66736

Smith SM, Jenkinson M, Woolrich MW, Beckmann CF, Behrens TE, Johansen-Berg H, Bannister PR, De Luca M, Drobnjak I, Flitney DE (2004) Advances in functional and structural MR image analysis and implementation as FSL. Neuroimage 23:S208–S219. https://doi.org/10.1016/j.neuroimage.2004.07.051

Stage E, Duran T, Risacher SL, Goukasian N, Do TM, West JD, Wilhalme H, Nho K, Phillips M, Elashoff D (2016) The effect of the top 20 Alzheimer disease risk genes on gray-matter density and FDG PET brain metabolism. Alzheimer's Dement 5:53–66

Stoffers D, Altena E, van der Werf YD, Sanz-Arigita EJ, Voorn TA, Astill RG, Strijers RL, Waterman D, Van Someren EJ (2014) The caudate: a key node in the neuronal network imbalance of insomnia? Brain 137(2):610–620. https://doi.org/10.1093/brain/awt329

Stoub T, Rogalski E, Leurgans S, Bennett D, deToledo-Morrell L (2010) Rate of entorhinal and hippocampal atrophy in incipient and mild AD: relation to memory function. Neurobiol Aging 31(7):1089–1098

Sudlow C, Gallacher J, Allen N, Beral V, Burton P, Danesh J, Downey P, Elliott P, Green J, Landray M (2015) UK biobank: an open access resource for identifying the causes of a wide range of complex diseases of middle and old age. PLoS Med 12(3):e1001779

Suri S, Heise V, Trachtenberg AJ, Mackay CE (2013) The forgotten APOE allele: a review of the evidence and suggested mechanisms for the protective effect of APOE ε2. Neurosci Biobehav Rev 37(10):2878–2886

Tan M-S, Yu J-T, Tan L (2013) Bridging integrator 1 (BIN1): form, function, and Alzheimer's disease. Trends Mol Med 19(10):594–603. https://doi.org/10.1016/j.molmed.2013.06.004

Tang X, Holland D, Dale AM, Younes L, Miller MI, AsDN I (2014) Shape abnormalities of subcortical and ventricular structures in mild cognitive impairment and Alzheimer's disease: detecting, quantifying, and predicting. Hum Brain Mapp 35(8):3701–3725. https://doi.org/10.1002/hbm.22431

Thompson PM, Hayashi KM, De Zubicaray GI, Janke AL, Rose SE, Semple J, Hong MS, Herman DH, Gravano D, Doddrell DM (2004) Mapping hippocampal and ventricular change in Alzheimer disease. Neuroimage 22(4):1754–1766

Thompson PM, Stein JL, Medland SE, Hibar DP, Vasquez AA, Renteria ME, Toro R, Jahanshad N, Schumann G, Franke B (2014) The ENIGMA Consortium: large-scale collaborative analyses of neuroimaging and genetic data. Brain Imaging Behav 8(2):153–182

van der Meer D, Frei O, Kaufmann T, Chen C-H, Thompson WK, O'Connell KS, Monereo Sánchez J, Linden DE, Westlye LT, Dale AM (2020) Quantifying the polygenic architecture of the human cerebral cortex: extensive genetic overlap between cortical thickness and surface area. Cereb Cortex 30(10):5597–5603

Veitinger M, Varga B, Guterres SB, Zellner M (2014) Platelets, a reliable source for peripheral Alzheimer's disease biomarkers? Acta Neuropathol Com 2(1):65. https://doi.org/10.1186/2051-5960-2-65

Walker KA, Hoogeveen RC, Folsom AR, Ballantyne CM, Knopman DS, Windham BG, Jack CR, Gottesman RF (2017) Midlife systemic inflammatory markers are associated with late-life brain volume: the ARIC study. Neurology 89(22):2262–2270. https://doi.org/10.1212/WNL.0000000000004688

Wang Y, Chan TF, Toga AW, Thompson PM (2009) Multivariate tensor-based brain anatomical surface morphometry via holomorphic one-forms. International conference on medical image computing and computer-assisted intervention. Springer, pp 337–344

Wang Y, Zhang J, Gutman B, Chan TF, Becker JT, Aizenstein HJ, Lopez OL, Tamburo RJ, Toga AW, Thompson PM (2010) Multivariate tensor-based morphometry on surfaces: application to mapping ventricular abnormalities in HIV/AIDS. Neuroimage 49(3):2141–2157

Wang Z-X, Wan Y, Tan L, Liu J, Wang H-F, Sun F-R, Tan M-S, Tan C-C, Jiang T, Tan L (2017) Genetic association of HLA gene variants with MRI brain structure in Alzheimer's disease. Mol Neurobiol 54(5):3195–3204. https://doi.org/10.1007/s12035-016-9889-z

Yao Z, Fu Y, Wu J, Zhang W, Yu Y, Zhang Z, Wu X, Wang Y, Hu B (2020) Morphological changes in subregions of hippocampus and amygdala in major depressive disorder patients. Brain Imaging Behav 14(3):653–667. https://doi.org/10.1007/s11682-018-0003-1

Zarei M, Patenaude B, Damoiseaux J, Morgese C, Smith S, Matthews PM, Barkhof F, Rombouts S, Sanz-Arigita E, Jenkinson M (2010) Combining shape and connectivity analysis: an MRI study of thalamic degeneration in Alzheimer's disease. Neuroimage 49(1):1–8

Zhang X, Yu J-T, Li J, Wang C, Tan L, Liu B, Jiang T (2015) Bridging integrator 1 (BIN1) genotype effects on working memory, hippocampal volume, and functional connectivity in young healthy individuals. Neuropsychopharmacology 40(7):1794–1803. https://doi.org/10.1038/npp.2015.30

Zhang W, Shi J, Stonnington C, Bauer RJ, Gutman BA, Chen K, Thompson PM, Reiman EM, Caselli RJ, Wang Y (2016) Morphometric analysis of hippocampus and lateral ventricle reveals regional difference between cognitively stable and declining persons. In: 2016 IEEE 13th International Symposium on Biomedical Imaging (ISBI). IEEE, pp 14–18